

Random network models with variable disorder of geometry

A. Klümper and W. Nuding

Bergische Universität Wuppertal, Gaußstraße 20, 42119 Wuppertal, Germany

A. Sedrakyan

*Yerevan Physics Institute, Br. Alikhanian 2, Yerevan 36, Armenia and
International Institute of Physics, Natal, Brazil*

(Dated: June 27, 2019)

Recently it was shown (I. A. Gruzberg, A. Klümper, W. Nuding and A. Sedrakyan, Phys. Rev. B 95, 125414 (2017)) that taking into account random positions of scattering nodes in the network model with $U(1)$ phase disorder yields a localization length exponent 2.37 ± 0.011 for plateau transitions in the integer quantum Hall effect. This is in striking agreement with the experimental value of 2.38 ± 0.06 . Randomness of the network was modeled by replacing standard scattering nodes of a regular network by pure tunneling resp. reflection with probability p where the particular value $p = 1/3$ was chosen. Here we investigate the role played by the strength of the geometric disorder, i.e. the value of p . We consider random networks with arbitrary probability $0 < p < 1/2$ for extreme cases and show the presence of a line of critical points with varying localization length indices having a minimum located at $p = 1/3$.

PACS numbers: 73.43.-f; 71.30.+h; 71.23.An; 72.15.Rn; 73.20.Fz

Introduction The physics of plateau transitions in the Integer Quantum Hall Effect (IQHE) poses a crucial condensed matter problem potentially necessitating a new understanding of quantum criticality. It relates not only to chiral systems where time reversal symmetry (TRS) is broken, but also to topological insulators (TI) with TRS. This transition is an example of a metal-insulator transition in two dimension where TRS is broken due to the presence of a magnetic field. In their seminal paper¹ Chalker and Coddington suggested a phenomenological model (CC model) for edge excitations in magnetic fields, where the disorder potential creates a scattering network based on quantum tunneling between Fermi levels of neighbor Fermi “puddles” in the ground state. For simplicity, the authors suggested that the scattering nodes in the landscape of the random potential are disposed regularly, while the information about randomness is coded in random $U(1)$ phases associated with the links of the network. During the last 30 years there were huge activities²⁻¹⁹ in understanding the CC model, its continuum limit and links to conformal field theories²⁰⁻²². A Spin Hall analog of the CC model was formulated²³ and investigated in²⁴. It appeared, however, that the position of scattering nodes on a regular lattice loses an essential part of the randomness of the potential. Numerical calculations of the Lyapunov exponent in the CC model give a localization length index $\nu = 2.56 \pm 0.011$ ²⁵⁻³⁰, which is well separated from the experimental value $\nu = 2.38 \pm 0.06$ ^{11,31,32}. Recently, alternatives to the CC model approach give values $\nu \simeq 2.58$ in Ref. [33] and $\nu = 2.48 \pm 0.02$ in [34] with only the latter being just compatible with the experimental result.

The discrepancy between the experimental value of ν and the CC model prediction may be due to the importance of electron-electron interactions studied in papers [35,36,37,38, 39]. However another solution of this prob-

lem was proposed in the paper⁴⁰, based on the observation that randomness of the relative positions of nearest neighbor scattering nodes has to be taken into account. For a depiction of a disorder potential with non-regular positioned saddle points see Fig. 1. This randomness of the network leads to the appearance of curvature in 2d space and may be regarded as the induction of quenched 2d gravity, which changes the universality class of the problem. In order to generate disordered networks in the transfer matrix formalism a new model was formulated, where the regular scattering with S -matrix $S = \begin{pmatrix} r & t \\ -t & r \end{pmatrix}$ at the saddle points is randomly replaced by two other extreme events. Here, the S -matrix takes the form of complete reflection, $(t, r) = (0, 1)$, with probability p_1 or the form of complete tunneling, $(t, r) = (1, 0)$, with probability p_2 as presented in Fig. 2. The probability of regular scattering events is $p_3 = 1 - p_1 - p_2$. The two extreme scattering events eliminate links in the scattering network. They perform a kind of “surgery” to a flat network where n -faces with $n = 3, 5, 6, \dots$ appear in the lattice. Examples of such “surgery” are presented in Fig. 2. Following this procedure we can formulate a hopping model of fermions on a random Manhattan lattice (ML), as is presented in Fig. 3, which corresponds to the landscape of the potential presented in Fig. 1.

The appearance of n -faces in the ML means, that our 2d geometry is not flat anymore and contains local Gaussian curvature $R_n = \frac{\pi}{2}(4 - n)$ for each n -face with $n \neq 4$. This is the discrete analog of the Gauss curvature integrated over a face $\int_{face} R \sqrt{g} d^2\xi$. Hence, the average over randomness of the saddle points leads to the average over all configurations of the curved space [41, 42], with yet to be determined functional measure. The field, which is characterizing different surfaces and by use of which one can ensure reparametrization invariance of the

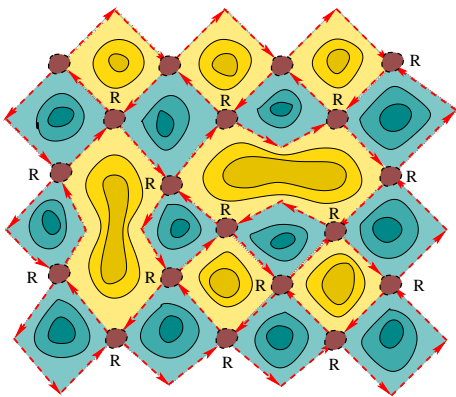


Figure 1. Modified CC network with two “open” nodes, one in the vertical and one in the horizontal direction.

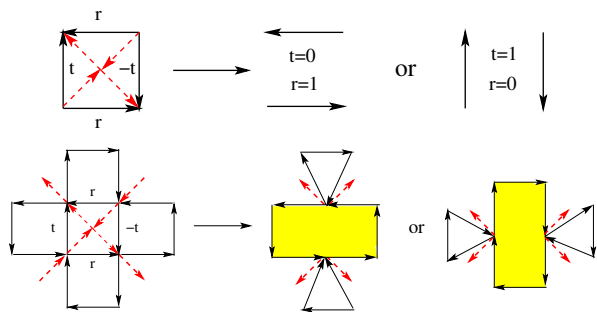


Figure 2. Top: Graphical illustration of the opening of a node. Bottom: The resulting modifications of the medial lattice.

model is the metric, while the corresponding theory is 2d gravity. This indicates that we have a non-critical string model, where all physical variables should be invariant under arbitrary coordinate transformations. The appearance of this new field and symmetry is the reason for the changes of the critical indices of the flat problem. And, as it appeared [40], by taking equal probability 1/3 for each of the three nodes (complete reflection, complete transmission, regular scattering), the localization length index becomes $\nu = 2.37 \pm 0.011$, very close to the experimental value. In passing, we like to remark that recently the problem of the fractional quantum Hall effect on arbitrary gravitational background has attracted considerable interest^{43–45}.

In papers Ref. [33, 34] the regular tight-binding lattice model in a magnetic field with random site energies was numerically analyzed. In [33] the authors considered the one particle Green’s function and got $\nu = 2.58(4)$ for the correlation length index, while in [34] the density of states around zero energy was analyzed yielding $\nu = 2.48 \pm 0.02$. The first paper confirms the result for the standard CC model. Our modified CC model differs essentially from this model because it contains information about the geometry of filled Landau levels, which form “lakes” in a random potential background. Assuming that the numerical analysis of both models was done on sufficiently large lattices we have to conclude that the

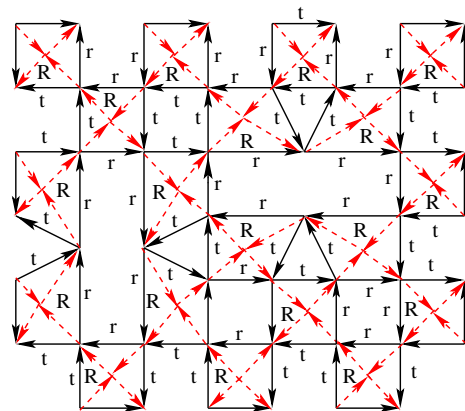


Figure 3. The modified medial lattice corresponding to the network shown in Fig. 1. We see two hexagons (vertically and horizontally oriented) appearing in neighborhood with two triangles each. Red dotted lines here correspond to red dotted lines in Fig.1.

models with different critical indices belong to different universality classes.

Another important question appearing here is the validity of the Harris criterion^{46,47}. According to it, for $d\nu > 2$ with d being the spatial dimension, any new disorder cannot change the critical index ν of the system. For the CC model we find $\nu \sim 2.56$ ^{25–30} so the above condition is fulfilled. Therefore one naively may expect, that disorder connected with randomness of the network cannot change the CC model localization length index.

The fundamental arguments leading to Harris criterion are based on the following observations, see for instance⁴⁸: We consider a system at some temperature T close to the critical temperature T_c of the ordered bulk. We then divide the space into correlated blocks of the size of the correlation length $\xi(T)$. Each block i has its own realization of disorder and has a corresponding transition temperature $T_{c,i}$. If the deviation of the critical temperatures, thanks to the central limit theorem of the order $\Delta T_i \sim \xi^{-d/2}$, is smaller than the distance of the actual temperature T from the critical point $T - T_c \sim \xi^{-1/\nu}$, then a uniform phase transition happens and the disorder is irrelevant. In the other case, different blocks may stay on different sides of the critical point T_c and far from it which will change the critical behavior. This is the case of geometric disorder involving a finite fraction of extreme nodes with $(t, r) = (0, 1)$ or $(t, r) = (1, 0)$ deviating considerably from the CC critical point $r_c = t_c = 1/\sqrt{2}$. In general, it appears questionable if the RG perturbative reasoning applies to strong disorder. Investigations concerning this issue are available⁴⁷. In summary, the presented arguments can not be considered as proof and the influence of geometric disorder on the applicability of Harris’ criterion needs further investigation.

A natural question that appears is, what is the meaning of probabilities p_i , $i = 1, 2, 3$ and do the critical indices of the model depend on them? In this paper we

consider the model with singular blocks (see Fig. 2b and Fig. 2c) appearing in the network with equal probabilities $p_1 = p_2 = p$, while the regular scattering has the probability $1 - 2p$. It is clear, that $p \leq 1/2$.

Construction and simulation of random networks.

For the calculation of the correlation length index of our model we used a variant of the transfer-matrix method formulated in Refs. [49, 50] and further developed in Ref. [1 and 26]. We calculate the product

$$\mathcal{T}_L = \prod_{j=1}^L T_{1j} U_{1j} T_{2j} U_{2j} \quad (1)$$

of layers of transfer matrices $M_1 U_{1j} M_2 U_{2j}$ corresponding to two columns T_{1j} and T_{2j} of vertical sequences of 2×2 scattering nodes,

$$T_{1j} = \begin{pmatrix} T_{\alpha_1}^1 & 0 & \dots & 0 \\ 0 & T_{\alpha_2}^1 & \dots & 0 \\ \vdots & \vdots & \ddots & \vdots \\ 0 & \dots & 0 & T_{\alpha_M}^1 \end{pmatrix} \quad (2)$$

and

$$T_{2j} = \begin{pmatrix} [T_{\alpha_1}^2]_{22} & 0 & \dots & 0 & [T_{\alpha_1}^2]_{21} \\ 0 & T_{\alpha_2}^2 & \dots & 0 & \vdots \\ \vdots & \vdots & \ddots & \vdots & \vdots \\ 0 & \dots & T_{\alpha_{M-1}}^2 & \dots & 0 \\ [T_{\alpha_1}^2]_{12} & 0 & \dots & 0 & [T_{\alpha_1}^2]_{11} \end{pmatrix}. \quad (3)$$

Here the index $\alpha_i = 1, 2, 3$ should be randomly fixed; $\alpha = 1$ with probability $1 - 2p$ for regular scatterings

$$T_1^1 = \begin{pmatrix} 1/t & r/t \\ r/t & 1/t \end{pmatrix}, \quad T_1^2 = \begin{pmatrix} 1/r & t/r \\ t/r & 1/r \end{pmatrix}, \quad (4)$$

or $\alpha = 2, 3$ with probability p , for ‘‘surgery’’ operations, i.e. ‘‘extremal scatterings’’

$$T_2^{1/2} = \begin{pmatrix} 1 & 0 \\ 0 & 1 \end{pmatrix}, \quad T_3^{1/2} = \begin{pmatrix} 1/\epsilon & \sqrt{1 - \epsilon^2/\epsilon} \\ \sqrt{1 - \epsilon^2/\epsilon} & 1/\epsilon \end{pmatrix}. \quad (5)$$

The parameter ϵ here is a regularization parameter, which ideally should be set to zero after the calculation of the Lyapunov exponent.

This choice of the transfer matrices corresponds to periodic boundary conditions in the transverse direction. In other words, these transfer matrices describe the random network model on a cylinder.

The U -matrices have a simple diagonal form with independent phase factors $U_{nm} = \exp(i\phi_n) \delta_{nm}$ for $U = U_{1j}$ and U_{2j} . The parameters t and r of the regular scattering are the transmission and reflection amplitudes at

each node and we parameterize them as in the previous paper [40]

$$t = \frac{1}{\sqrt{1 + e^{2x}}} \quad \text{and} \quad r = \frac{1}{\sqrt{1 + e^{-2x}}}. \quad (6)$$

The parameter x corresponds to the Fermi energy measured from the Landau band center scaled by the Landau band width. Following paper [40] we expect that the critical point of the model of arbitrary p is still given by the value $t_c^2 = 1/2$ as for the regular nodes corresponding to $x = 0$. The phases ϕ_n are random variables uniformly distributed in the range $[0, 2\pi)$, reflecting that the phase of an electron approaching a saddle point of the random potential is arbitrary.

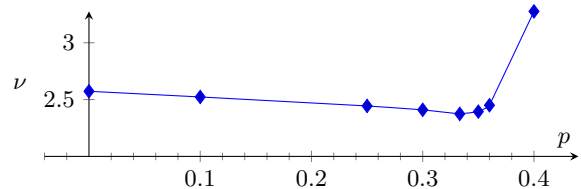


Figure 4. Localization length index ν_p versus probability p of singular blocks

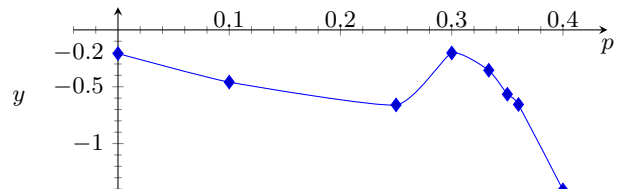


Figure 5. Subleading index versus probability p of singular blocks

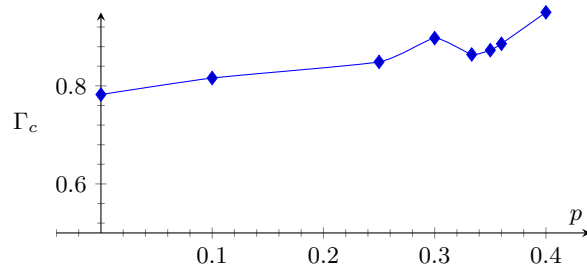


Figure 6. Coefficient $\Gamma_c = \pi(\alpha_0 - 2)$ related to the multifractal exponent α_0 versus probability p of singular blocks

To extract the exponent ν for random networks, we numerically estimate the Lyapunov exponent γ defined as the smallest positive eigenvalue of

$$\frac{1}{2L} \log[T_L T_L^\dagger]. \quad (7)$$

in the limit $L \rightarrow \infty$. In the standard transfer matrix method one multiplies many transfer matrices for a single realization of disorder and relies on the self-averaging

property of Lyapunov exponents. This property in the limit of infinite length of the sample is the subject of the central-limit-type theorem for products of random matrices due to Oseledec.⁵¹ The modification of Ref. [26] that we use here, however, is based on another central-limit-type theorem for products of random matrices due to Tutubalin.⁵² This theorem states that the Lyapunov exponents of products of a finite number of random matrices are random numbers whose distribution approaches Gaussian for large sample lengths.

These theorems allow us to simulate ensembles of $N_r = 624$ strips of height M (the number of nodes per column, varying from 20 to 200) in the case of $q = 1/3$ and length $L = 5 \cdot 10^6$. This is equivalent²⁶ to the standard transfer matrix simulation of a single sample of effective length $L_{\text{eff}} = N_r \times L > 3 \cdot 10^9$, exceeding the longest previously reported sample lengths. Moreover this method allows for an estimate of the precision of the calculated Lyapunov exponents by means of the standard deviation of those ensembles. The range of the parameter x we have considered is $x \in [0, 0.08]$ which encodes deviations of t from t_c . Then we fit all data of the Lyapunov exponent for pairs of the parameters (M, x) extracting the localization index ν . For each ensemble of the random network we check that the histogram of the Lyapunov exponents is close to a Gaussian.

We use the so-called LU decomposition of transfer matrices³⁰, because it is faster than the standard QR decomposition approach. Since t and r appear in the denominators of the matrix elements of transfer matrices, making them zero is a singular procedure, related to the disappearance of two horizontal channels upon opening a node in the vertical direction (see Fig. 2). To overcome this difficulty, following [40] we take for every open node either t or r to be equal to $\varepsilon \ll 1$. It appears, that the result for the Lyapunov exponent is unchanged within our error 10^{-3} in a range from $\varepsilon = 10^{-5}$ up to ε to 10^{-7} . For even smaller ε the results start changing again. This is to be expected because the large differences of values in the entries of transfer matrices cause numerical instabilities for the LU decomposition. Interestingly, we found that the results for the Lyapunov exponents for longer chains depend less on the value of ε than for shorter chains. We have chosen $\varepsilon = 10^{-6}$ for our calculations.

As usual, the Lyapunov exponent γ is expected to have the following finite-size scaling behavior:

$$\gamma M = \Gamma[M^{1/\nu} u_0(x), M^y u_1(x)]. \quad (8)$$

Here $u_0(x)$ is the relevant field and $u_1(x)$ is the leading irrelevant field. The relevant field vanishes at the critical point, and $y < 0$. The fitting and the error analysis of our numerical data are described in the appendices. The results of the analysis as functions of the disorder parameter p are presented in Fig. 4 for the localization length exponent ν , in Fig. 5 for the exponent y of the irrelevant field and in Fig. 6 for the parameter $\Gamma_c = \pi(\alpha_0 - 2)$ related to the multifractal exponent α_0 . In table I we present these results as numbers.

p	Γ_c	$\Delta\Gamma_c$	ν	$\Delta\nu$	y	Δy
0	0.7823	0.05695	2.573	0.0145	-0.2078	0.3744
0.1	0.816	0.00595	2.523	0.0213	-0.4592	0.1089
0.25	0.8489	0.00295	2.444	0.017	-0.6598	0.0527
0.3	0.8974	0.07275	2.41	0.027	-0.2028	0.0588
1/3	0.864	0.864	2.374	0.0175	-0.355	0.05
0.35	0.8728	0.04895	2.394	0.015	-0.5661	1.7
0.36	0.8859	0.04395	2.45	0.0395	-0.6562	1.9235
0.4	0.95	0.00465	3.276	0.082	-1.408	0.6487

Table I. Numerical values for the exponents ν , y and the multifractal parameter Γ_c and their uncertainties. Different cases of the disorder parameter $p \in [0, 1[$ are considered.

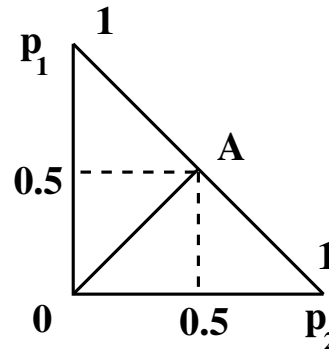


Figure 7. The (p_1, p_2) phase diagram of the model ($p_1 + p_2 \leq 1$). The segment $[0, A]$ is a line of critical points.

Fig. 4 shows an interesting behavior of ν versus the probability p . We see that a minimum is achieved precisely at $p = 1/3$ which may very likely correspond to the plateau transitions in IQHE. The value $p = 0$ gives $\nu = 2.56$ for the Chalker-Coddington model, just as expected. At $p = 1/2$, where we do not have regular scattering nodes at all the x dependence of γ should disappear. Therefore, one can expect $\nu = \infty$, because precisely in this situation the critical behavior of the Lyapunov exponent of the form x^ν will produce zero. As we see from Fig. 4, the index sharply increases close to $p = 1/2$.

Results and summary.

In summary, we have considered the possibility that a certain type of geometric disorder, previously missing in the study of the integer QH transition, changes its universality class. Our numerical simulations support this idea. We see that the random occurrence of singular blocks in the network with some probability p leads to a geometry with curvature. The network model has a critical index ν_p that apparently changes continuously with p , i.e. it realizes a line of critical points with different universality classes at different points. The $p_1 - p_2$ phase diagram of the model is presented in Fig. 7, where the diagonal line from zero to A is a line of critical points.

The minimal value of ν at $p = 1/3$ corresponds to the value expected for the exponent of the IQH transitions. The meaning of the other models as well as the mean-

ing of the parameter p remains an open question at the moment. It would be not surprising, if the approaches presented in papers [33] and [34] were related to different parameters p in our model.

ACKNOWLEDGMENTS

A. S. was supported by ARC grants 18T-1C153 and 18RF-039. A. K. acknowledges financial support by DFG. The authors are grateful to I. A. Gruzberg for many stimulating discussions and valuable comments.

-
- ¹ J. T. Chalker and P. D. Coddington, *J. Phys. C* **21**, 2665 (1988).
- ² B. Huckestein, *Rev. Mod. Phys.* **67**, 357 (1995).
- ³ B. Huckestein, *Europhys. Lett.* **20**, 451 (1992).
- ⁴ B. Huckestein, *Phys. Rev. Lett.* **72**, 1080 (1994).
- ⁵ D.-H. Lee, Z. Wang, and S. Kivelson, *Phys. Rev. Lett.* **70**, 4130 (1993).
- ⁶ A. W. W. Ludwig, M. P. A. Fisher, R. Shankar, and G. Grinstein, *Phys. Rev. B* **50**, 7526 (1994).
- ⁷ K. Yang and R. N. Bhatt, *Phys. Rev. Lett.* **76**, 1316 (1996).
- ⁸ C. de C. Chamon, C. Mudry, and X.-G. Wen, *Phys. Rev. B* **53**, 7638 (1996).
- ⁹ D.-H. Lee and Z. Wang, *Phys. Rev. Lett.* **76**, 4014 (1996).
- ¹⁰ R. Klesse and M. Metzler, *Europhys. Lett.* **32**, 229 (1995).
- ¹¹ W. Li, G. A. Csáthy, D. C. Tsui, L. N. Pfeiffer, and K. W. West, *Phys. Rev. Lett.* **94**, 206807 (2005).
- ¹² M. R. Zirnbauer, arXiv eprint (1999), hep-th/9905054.
- ¹³ M. R. Zirnbauer, *J. Math. Phys.* **37**, 4986 (1996).
- ¹⁴ M. R. Zirnbauer, *Annalen Phys.* **3**, 513 (1994), [Erratum: *Annalen Phys.* **4**, 89 (1995)].
- ¹⁵ A. G. Galstyan and M. E. Raikh, *Phys. Rev. B* **56**, 1422 (1997).
- ¹⁶ P. Cain, R. Römer, and M. E. Raikh, *Phys. Rev. B* **67**, 075307 (2003).
- ¹⁷ V. V. Mkhitarian and M. E. Raikh, *Phys. Rev. B* **79**, 125401 (2009).
- ¹⁸ V. V. Mkhitarian, V. Kagalovsky, and M. E. Raikh, *Phys. Rev. Lett.* **103**, 066801 (2009).
- ¹⁹ J. Song and E. Prodan, *Euro. Phys. Lett.* **105**, 37001 (2014).
- ²⁰ M. J. Bhaseen, I. I. Kogan, O. A. Soloviev, N. Taniguchi, and A. M. Tsvelik, *Nucl. Phys. B* **580**, 688 (2000).
- ²¹ A. M. Tsvelik, arXiv eprint (2001), cond-mat/0112008.
- ²² A. LeClair, *Phys. Rev. B* **64**, 045329 (2001).
- ²³ V. Kagalovsky, B. Horowitz, Y. Avishai, and J. T. Chalker, *Phys. Rev. Lett.* **82**, 3516 (1999).
- ²⁴ I. A. Gruzberg, A. W. W. Ludwig, and N. Read, *Phys. Rev. Lett.* **82**, 4524 (1999).
- ²⁵ K. Slevin and T. Ohtsuki, *Phys. Rev. B* **80**, 041304 (2009).
- ²⁶ M. Amado, A. V. Malyshev, A. Sedrakyan, and F. Domínguez-Adame, *Phys. Rev. Lett.* **107**, 066402 (2011).
- ²⁷ K. Slevin and T. Ohtsuki, *Int. J. Mod. Phys. Conf. Ser.* **11**, 60 (2012).
- ²⁸ H. Obuse, I. A. Gruzberg, and F. Evers, *Phys. Rev. Lett.* **109**, 206804 (2012).
- ²⁹ J. P. Dahlhaus, J. M. Edge, J. Tworzydło, and C. W. J. Beenakker, *Phys. Rev. B* **84**, 115133 (2011).
- ³⁰ W. Nuding, A. Klümper, and A. Sedrakyan, *Phys. Rev. B* **91**, 115107 (2015).
- ³¹ H. P. Wei, L. W. Engel, and D. C. Tsui, *Phys. Rev. B* **50**, 14609 (1994).
- ³² W. Li, C. L. Vicente, J. S. Xia, W. Pan, D. C. Tsui, L. N. Pfeiffer, and K. W. West, *Phys. Rev. Lett.* **102**, 216801 (2009).
- ³³ M. Puschmann, M. Cain, M. Schreiber, and T. Vojta, *Phys. Rev. B* **99**, 121301 (2019).
- ³⁴ Q. Zhu, P. Wu, R. Bhatt, and X. Wan, *Phys. Rev. B* **99**, 024205 (2019).
- ³⁵ D. G. Polyakov and B. I. Shklovskii, *Phys. Rev. Lett.* **70**, 3796 (1993).
- ³⁶ A. M. M. Pruisken and M. A. Baranov, *Europhysics Letters* **31**, 543 (1995).
- ³⁷ A. M. M. Pruisken and I. S. Burmistrov, *J. Exp. Theor. Phys. Lett.* **220** (2008).
- ³⁸ Z. Wang, M. P. A. Fisher, S. M. Girvin, and J. T. Chalker, *Phys. Rev. B* **61**, 8326 (2000).
- ³⁹ I. S. Burmistrov, S. Bera, F. Evers, I. V. Gornyi, and A. D. Mirlin, *Annals of Physics* **326**, 1457 (2011).
- ⁴⁰ I. Gruzberg, W. Nuding, A. Kluemper, and A. Sedrakyan, *Phys. Rev. B* **95**, 125414 (2017).
- ⁴¹ J. Ambjörn and A. Sedrakyan, *Nucl. Phys. B* **874** [PM], 877888 (2015).
- ⁴² J. Ambjörn, K. Sh., and A. Sedrakyan, *Phys. Rev. D* **92**, 026002 (2015).
- ⁴³ T. Can, M. Laskin, and P. Wiegmann, *Phys. Rev. Lett.* **113**, 046803 (2014).
- ⁴⁴ T. Can, M. Laskin, and P. Wiegmann, *Ann. Phys.* **362**, 752 (2015).
- ⁴⁵ M. Laskin, T. Can, and P. Wiegmann, *Phys. Rev. B* **92**, 235141 (2015).
- ⁴⁶ A. B. Harris, *J. Phys. C* **7**, 1671 (1974).
- ⁴⁷ J. T. Chayes, L. Chayes, D. S. Fisher, and T. Spencer, *Phys. Rev. Lett.* **57**, 2999 (1986).
- ⁴⁸ T. Vojta, *Lectures on the Physics of Strongly Correlated Systems XVII AIP Conf. Proc.* **1550**, 188 (2013).
- ⁴⁹ A. MacKinnon and B. Kramer, *Phys. Rev. Lett.* **47**, 1546 (1981).
- ⁵⁰ A. MacKinnon and B. Kramer, *Z. Phys. B* **53**, 1 (1983).
- ⁵¹ V. I. Oseledec, *Trudy Moskov. Mat. Obsč.* **19**, 179 (1968).
- ⁵² V. Tutubalin, *Theory Probab. Appl.* **10**, 15 (1965).
- ⁵³ H. Obuse, A. R. Subramaniam, A. Furusaki, I. A. Gruzberg, and A. W. W. Ludwig, *Phys. Rev. B* **82**, 035309 (2010).
- ⁵⁴ H. Akaike, *IEEE Trans. Automat. Control* **19**, 716 (1974).

SUPPLEMENTAL MATERIAL

The fitting procedure

As is standard in the transfer matrix method, we want to numerically estimate the Lyapunov exponent γ defined

as the smallest positive eigenvalue of

$$\frac{1}{2L} \log[T_L T_L^\dagger]. \quad (1)$$

in the limit as $L \rightarrow \infty$. This quantity is self-averaging, and for finite L its distribution is basically Gaussian. This is illustrated for a particular set of parameters M, X, p in Fig. 8.

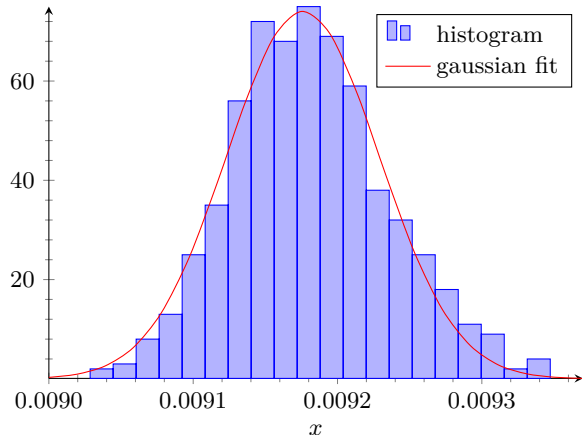


Figure 8. Distribution of Lyapunov exponents in the ensemble of 624 realizations for chain length $L = 5\,000\,000$, block size $M = 100$, parameter $x = 0.04$, and disorder parameter $p = 1/4$.

We numerically calculated γ for various combinations of the parameter x and the lattice width M . The results are shown in Fig. 9.

It is clearly seen that the lines corresponding to different values of M do not intersect at the critical value $x = 0$. In fact, they do not intersect at a single point at all. Therefore, any attempt at trying to use a single-parameter scaling to collapse the data is doomed to fail. The reason for this is that the critical point of the CC model is not the same as the fixed point. They differ by the presence of irrelevant variables that decay as we increase the system width. For the CC model specifically, the leading irrelevant variable has the scaling exponent $y < 0$ which is rather small in magnitude. This causes strong correction to scaling even at the critical point. This is a known feature of the CC model that has been stressed by Slevin and Ohtsuki in Ref. [25]. They emphasized that it is crucial to include irrelevant scaling variables as arguments of the fitting functions used in the scaling analysis of the data. This procedure leads to much more reliable results, but cannot be visualized as a simple scaling collapse of the numerical data, as in the case of a single-variable scaling. Inclusion of irrelevant variables in the scaling analysis has become a standard procedure in the numerical studies of network models, and here we follow the same procedure.

Thus, we fit the scaling behavior of the Lyapunov exponent γ near the critical point to the following expression:

$$\gamma \cdot M = \Gamma(M^{1/\nu} u_0, M^y u_1), \quad (2)$$

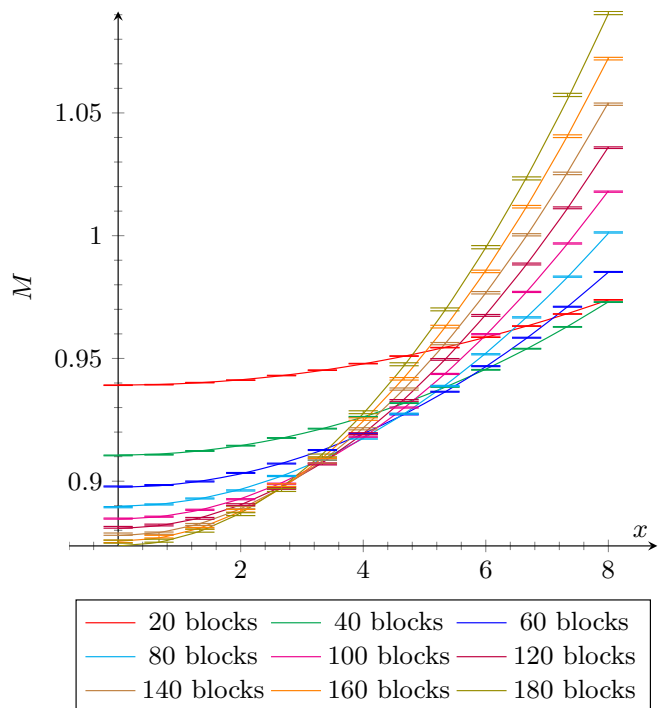


Figure 9. Plot of the logarithm of the smallest eigenvalue of the transfer matrix times M ($=$ number of blocks) depending on the distance x from the critical point for the model with disorder parameter $p = 1/4$. The x -values divide the interval $[0, 0.08]$ into 12 equal parts. The data points are given by the average of the ensemble belonging to the corresponding values for x and M . All considered values for M are listed in the legend. The product length is $L = 5\,000\,000$. The error bars are obtained from the standard deviation of this ensemble. The curves are obtained by plotting the fit function for the relevant values of M in the regime $x = 0$ to $x = 0.08$. The ensembles vary between 208 and 1096 eigenvalues. Details on the ensemble sizes can be found in appendix A

Here we have taken into account the relevant field with exponent ν and the leading irrelevant field with exponent y . M is the number of 2×2 blocks in the transfer matrices ($=$ half the number of horizontal channels of the lattice), $u_0 = u_0(x)$ is the relevant field and $u_1 = u_1(x)$ the leading irrelevant field. It is known that the relevant field vanishes at the critical point, and that $y < 0$.

Regarding the two-variable fit, on the left hand side of Eq. (2) we use the numerical results for the eigenvalues of T_L , where we are particularly interested in the eigenvalue closest to 1. The right hand side of (2) is expanded in a series in x and powers of M , and the expansion coefficients are obtained from a fit. Some coefficients in this expansion vanish due to a symmetry argument.²⁵ If x is replaced by $-x$ we see from (6) that t turns into r and vice versa. Due to the periodic boundary conditions the lattice is unchanged. Therefore the left hand side of (2) is invariant under the sign change of x . Hence the right hand side must be even in x . That renders $u_0(x)$ and $u_1(x)$ either even or odd in x . For the Chalker Codding-

ton network the critical point is at $x = 0$. This lets us choose $u_0(x)$ odd and $u_1(x)$ even. The fit now should use as few coefficients as possible while reproducing the data as closely as possible.

The scaling function Γ in the right side of (2) is expanded in the fields u_0 and u_1 yielding

$$\begin{aligned} \Gamma(u_0(x)M^{1/\nu}, u_1(x)M^y) = & \Gamma_c + \Gamma_{01}u_1M^y + \Gamma_{20}u_0^2M^{2/\nu} \\ & + \Gamma_{02}u_1^2M^{2y} + \Gamma_{21}u_0^2u_1M^{2/\nu}M^y + \Gamma_{03}u_1^3M^{3y} \\ & + \Gamma_{40}u_0^4M^{4/\nu} + \Gamma_{22}u_0^2M^{2/\nu}u_1^2M^{2y} + \Gamma_{04}u_1^4M^{4y} + \dots \end{aligned} \quad (3)$$

We further expand u_0 and u_1 in powers of x as was done, for example, in Refs. [25, 26]:

$$u_0(x) = x + \sum_{k=1}^{\infty} a_{2k+1}x^{2k+1} \quad \text{and} \quad u_1(x) = 1 + \sum_{k=1}^{\infty} b_{2k}x^{2k}. \quad (4)$$

In Eq. (3) we retained only terms that are even in x . Because of the ambiguity in the overall scaling of the fields, the leading coefficient in Eq. (4) can be chosen to be 1.

The first term in the expansion (3), Γ_c represents the asymptotic value of the universal critical amplitude ratio Γ in the infinite system. Theoretical arguments based on conformal invariance relate Γ to the multifractal exponent α_0 :

$$\Gamma_c = \pi(\alpha_0 - 2), \quad (5)$$

see, for example, Ref. [53].

Weights and Errors

The left hand side of Eq. (2) is determined by the results of numerical simulations of the random network model. Following Ref. [26] we have produced large ensembles of the Lyapunov exponent γ for a variety of choices for the probability index p by simulating many disorder realizations for many combinations of x and M . We calculated disorder realizations for any combination of $M = 20, 40, 60, 80, 100, 120, 140, 160, 180, 200$ and $x = 0.08/12 \cdot [0, 1, 2, 3, 4, 5, 6, 7, 8, 9, 10, 11, 12]$ for fixed $L = 5\,000\,000$. Details on the ensemble sizes can be found in appendix A. Our goal is to check whether the central limit theorem⁵² also works in the case of randomness of the network or not. Fig. 8 shows the distribution of the Lyapunov exponent for $p = 1/4$, $M = 100$ and $x = 0.04$ being nicely described by a Gaussian which demonstrates the validity of the central limit theorem.

In the fitting procedure, the weight of each such γ is given by the reciprocal of the variance of the corresponding ensemble. So all γ from the same (x, M) ensemble enter the fit with the same weight. On the right hand side of Eq. (2) the fitting formula (3) depending on x

and M is used. The coefficients of the expansion and the critical exponents are the fitting coefficients.

The fits are performed in several steps. First a weighted nonlinear least square fit based on a trust region algorithm with specified regions for each parameter is applied. The resulting parameters are used in a further weighted nonlinear least square fit based on a trust region algorithm. Here no limits are imposed on the fit parameters. The last step is repeated until the resulting parameters stop changing.

Evaluation of fits

There are several methods for the evaluation of the fit results.

The χ^2 -test with χ^2 given by

$$\chi^2 = \sum_i \frac{(y_i - f_i)^2}{\sigma_i^2} \quad (6)$$

where f_i is the value obtained by the fit function and y_i is the measured value. The parameters σ_i are the standard deviations of the ensemble i with values for (x_i, M_i) . Our fit contains a large ensemble of data points for each (x_i, M_i) coordinate. Hence $\chi^2 = 0$ is not possible, in fact it will be large due to the huge number of data points. Therefore, we consider the ratio $\chi^2/\text{degrees of freedom}$ with expectation value 1 in case of an ideal fit. The *degrees of freedom* equals the number of data points in the fit minus the number of fit parameters.

Deviations from 1 are evaluated by use of the cumulative probability $P(\tilde{\chi}^2 < \chi^2)$ which is the probability of observing a sample statistic with a smaller χ^2 value than in our fit. A small value of P , and hence a large value of the complement $Q := 1 - P$ is indicative for a good fit. Yet, values of P lower than 1/2 would indicate problems in the estimation of error bars of the individual data points.

Another criterion uses the width of the *confidence intervals* which quantifies the quality of the prediction for a single parameter. We use 95% confidence intervals meaning that for repeated independent generations of the data and subsequent data analysis, the resulting confidence intervals contain the true parameter values in 95% of the cases.

A very sensitive criterion is the *Akaike information criterion* (AIC)⁵⁴ which allows to select between model fit functions. Suppose, we have l models with $\text{AIC}_1, \dots, \text{AIC}_l$. The model with the smallest AIC is the favorite one: The relative probability of model j compared to the model with minimum AIC_{\min} is

$$\exp \frac{\text{AIC}_{\min} - \text{AIC}_j}{2}, \quad (7)$$

which is always smaller than one.

The last criterion we present is the sum of *residuals* which is given by $\text{res} = \sum_j \text{res}_j$, $\text{res}_j = y_j - f_j$. The condition is that res be small compared to the number of degrees of freedom.

Appendix A: Tables of ensemble statistics

In this appendix we present the statistics of our data sets. For each p we present a table showing the number of Lyapunov exponents for each (x, M) pair. As explained in the introduction, p is the probability for enforced horizontal respectively vertical transition in the network and $1 - 2p$ is the probability for regular scattering.

$p = 0$ (Classical Chalker Coddington Lattice³⁰)

M	x													L
	0	0.0067	0.0133	0.0200	0.0267	0.0333	0.0400	0.04667	0.0533	0.0600	0.0667	0.0733	0.0800	
20	208	208	208	208	208	208	208	208	208	208	208	208	208	5000000
40	152	152	304	152	152	0	152	152	152	152	152	152	152	5000000
60	208	208	208	208	208	208	208	208	208	208	208	208	208	5000000
80	208	208	208	208	208	208	208	208	208	208	208	208	208	5000000
100	208	200	200	200	200	200	200	200	200	200	208	200	200	5000000
120	150	150	296	146	148	0	150	152	150	150	152	150	150	5000000
140	208	208	208	208	208	208	208	208	208	208	208	208	208	5000000
160	208	176	144	144	176	112	144	192	192	144	128	144	128	5000000
180	208	208	208	208	208	208	208	208	208	208	208	208	208	5000000

$p = 0.1$

M	x													L
	0	0.0067	0.0133	0.0200	0.0267	0.0333	0.0400	0.04667	0.0533	0.0600	0.0667	0.0733	0.0800	
20	384	384	384	384	384	384	400	400	400	400	400	400	400	5000000
40	224	208	208	208	208	208	208	208	208	208	208	208	208	5000000
60	208	208	208	208	208	208	208	208	208	208	208	208	208	5000000
80	208	208	208	208	208	208	208	208	208	208	208	208	208	5000000
100	208	208	208	208	208	208	208	208	208	208	208	208	208	5000000
120	208	208	208	208	208	208	208	208	208	208	208	208	208	5000000
140	176	240	240	256	272	272	272	256	240	272	224	256	192	5000000
160	208	208	208	208	208	208	208	208	208	208	208	208	208	5000000
180	256	288	288	288	272	272	272	272	272	272	288	288	288	5000000
200	416	416	400	416	400	368	384	400	400	384	400	368	416	5000000

$p = 0.35$

M	x													L
	0	0.0067	0.0133	0.0200	0.0267	0.0333	0.0400	0.04667	0.0533	0.0600	0.0667	0.0733	0.0800	
20	208	208	192	208	192	208	208	192	208	208	192	208	208	5000000
40	208	208	208	208	208	208	208	208	208	208	208	208	208	5000000
60	208	208	208	208	208	208	208	208	208	192	192	208	192	5000000
80	208	192	208	208	208	208	192	208	208	192	208	208	208	5000000
100	192	192	176	192	176	192	144	176	192	208	192	160	192	5000000
120	208	208	192	208	208	208	208	208	208	192	208	208	208	5000000
140	208	208	208	208	192	208	192	208	208	208	208	208	208	5000000
160	208	176	192	160	192	192	192	176	176	176	176	160	208	5000000
180	400	416	416	416	416	384	416	416	416	416	416	416	416	5000000
200	208	208	208	208	208	208	208	208	208	208	208	208	208	5000000

 $p = 0.36$

M	x													L
	0	0.0067	0.0133	0.0200	0.0267	0.0333	0.0400	0.04667	0.0533	0.0600	0.0667	0.0733	0.0800	
20	192	176	192	144	160	192	192	192	192	208	208	192	160	5000000
40	208	208	208	208	208	208	208	208	208	208	208	208	208	5000000
60	208	208	208	208	208	208	208	192	208	208	208	208	208	5000000
80	208	208	208	208	208	208	208	208	208	192	208	208	208	5000000
120	208	208	208	208	208	208	208	208	208	208	208	208	208	5000000
160	208	208	208	208	208	208	208	208	208	208	208	208	208	5000000
200	208	192	192	208	208	208	208	208	192	192	208	208	192	5000000

 $p = 0.4$

M	x													L
	0	0.0067	0.0133	0.0200	0.0267	0.0333	0.0400	0.04667	0.0533	0.0600	0.0667	0.0733	0.0800	
20	416	416	416	416	416	416	416	416	416	416	416	416	416	5000000
40	416	416	416	416	416	416	416	416	416	416	416	416	416	5000000
60	416	416	416	416	416	416	416	416	416	416	416	416	416	5000000
80	208	208	208	208	208	208	208	208	208	208	208	208	208	5000000
100	208	208	208	208	208	208	208	208	208	208	208	208	208	5000000
120	208	208	208	208	208	208	208	208	208	208	208	208	208	5000000
140	208	208	208	208	208	208	208	208	208	208	208	208	208	5000000
160	208	208	208	208	208	208	208	208	208	208	208	208	208	5000000
180	208	208	208	192	208	192	208	192	208	208	208	208	208	5000000